Article ID: 1003－6326(2004)03－0510－06

Characterization of phase transformation and microstructure of nano hard phase Ti(C, N)-based cermet by spark plasma sintering①

FENG Ping(丰 平)[1, 2], XIONG Wei-hao(熊惟皓)[1], LI Peng(李 鹏)[1],
YU Li-xin(余立新)[1], XIA Yang-hua(夏阳华)[1]
(1. State Key Laboratory of Die & Mould Technology,
Huazhong University of Science and Technoloty, Wuhan 430074, China;
2. Department of Mechanical & Materials Engineering,
China Three Gorges University, Yichang 443002, China)

Abstract: By means of optical microscope (OM), scanning electron microscope (SEM) and transmission electron microscope (TEM), the process of densification, the characterization of phase transformation and the microstructure for spark plasma sintering (SPS) nano hard phase Ti(C, N)-based cermet were investigated. It is found that the spark plasma sintering (SPS) enables the nano hard phase Ti(C, N)-based cermet to densify rapidly, however, the full densification of the sintered samples can not be obtained. The rate of phase transformation is significantly quick. When being sintered at 1 200 ℃ for 8 min, Mo_2C is completely dissolved, and TiN dissolves into TiC entirely and disappears. Above 1 200 ℃, Ti(C, N) begins to decompose and the atoms of C and N separate from Ti(C, N) resulting in the generation of N_2 and the graphite. Due to the denitrification and the graphitization, the density and the hardness of sintered samples are rather low. The distribution of grain size of the sample sintered at 1 350 ℃ covers a wide range of 90－500 nm, and most of the grain size are about 200 nm. The hard phase is not of typical core-rim structure. Oxides on the surface of particles can not be fully removed and present in sample as titanium oxide TiO_2. Graphite exists in band-like shape.

Key words: Ti(C, N)-based cermet; nano phase; spark plasma sintering; phase transformation; microstructure
CLC number: TG 148 **Document code:** A

1 INTRODUCTION

Spark plasma sintering(SPS) is a comparatively new technique. It has many merits compared with conventional sintering methods, for example, superfast heating and cooling rate, transient and low temperature sintering to gain fully dense product. Moreover, during the early sintering stage, the spark plasma generated among the gaps of particles can purify the surface of particles and availably improve the sinterablity of powders[1-3]. Especially SPS reveals a powerful potential on fabricating fine grained and nano structured materials[4-7], and the low temperature and short period sintering facilitate the control of nano particles. In recent years, SPS has been successfully applied to prepare novel materials and to improve the structures and properties of traditional materials such as ceramics[8], composite materials[9, 10], metals[11] and alloys[12].

Ti(C, N)-based cermets have series of unique properties compared with conventional WC-base hardmetals and even with coated hardmetals, and they have been successfully introduced in metal cutting industry. The grain size has been decreased from micron order to sub-micron and ultrafine order in microstructure[13-15]. However, it has not yet reported on fabrication of nano-structural Ti(C, N)-based cermets. Since nano-sized carbides rapidly dissolved to binder and precipitated from binder, it was very difficult to prepare nano-structural Ti(C, N)-based cermets by conventional sintering methods. In present work, SPS was used to fabricate nano-structured Ti(C, N)-based cermets under lower temperature, and the particularities for SPS nano hard phase Ti(C, N)-based cermet were investigated, such as the process of densfication and the characterization of phase transformation and microstructure.

2 EXPERIMENTAL

Commercially available powders were used. Nano-sized hard phase powders of TiC and TiN were employed in present work. Fig. 1 presents the TEM images of nano TiC and TiN particles. The mean particle size and oxygen content of used powders are list-

① **Foundation item:** Project(50074017) supported by the National Natural Science Foundation of China; Project supported by the State Key Laboratory of Advanced Technology for Materials Synthesis and Processing of Wuhan University of Technology, China
Received date: 2003－11－22; **Accepted date:** 2004－01－30
Correspondence: FENG Ping, PhD; E-mail: feng.ping@263.net

ed in Table 1.

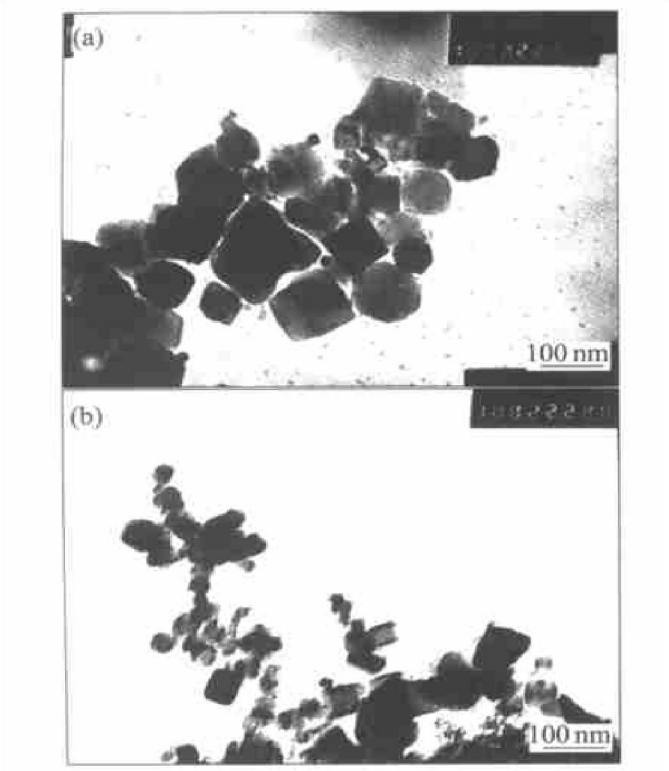

Fig. 1 TEM images showing morphology and size of nano particles
a) —Nano TiC; b) —Nano TiN

Table 1 Particle size and oxygen content of powders employed in SPS

Ingredient	Mean particle size/ μm	Oxygen content(mass fraction) / %	Purity/ %
nano TiC	< 0.09	1.08	
nano TiN	< 0.04	5.23	
Mo	2.8	0.1	
Ni	2.18	0.22	
C			> 99.85

The composition of prepared Ti(C, N)-based cermet was designated as TiC-23TiN-11.28Mo-0.72C-12Ni(mass fraction, %). Extra double content free C was added to reduce oxygen on the surface of powder. All ingredients were wetly mixed for 48 h in nylon vial on planetary ball mill, where alcohol was used as dispersant media and WC-Co as ball milling media. The slurry was dried under 80 ℃.

SPS was conducted on Dr Sinter 1050 SPS (Sumitomo Coal Mining Co.). Different SPS processes was adopted. The heating rate was 200 ℃/ min and the sintered sample was cooled down to 700 ℃ within 2 – 3 min. The pressure of 30 MPa was maintained during the whole sintering. The sintering processing parameters are listed in Table 2.

Table 2 SPS processing parameters

Sintering temperature/ ℃	1 050	1 050	1 200	1 350	1 430
Dwelling time/ min	3	8	8	8	8

The preparation of specimen and observation for porosity were in accordance with ISO4505. X-ray diffraction(XRD) analysis was carried out on D/MAX-RB X-ray diffractometer to identify present phases in the mixed powders and samples sintered at different SPS processes. Transmission electron microscope(TEM) and selected area electron diffraction patterns(SED) were essential supplement for more accurate phase identification. TEM and SED were conducted on JEM-2000FX Ⅱ.

The microstructure was observed using JSM-5610LV scanning electron microscope(SEM) in back-scattered electron imaging.

3 RESULTS AND DISCUSSION

3.1 Densification process

Due to the change of chemical compositions during sintering, the densification process was investigated in present work. Fig. 2 presents metallographs of samples sintered at various temperatures.

From Fig. 2, it was found that remarkable densification had occurred in sintering at 1 050 ℃ for 3 min, and fine pores uniformly distributed over the sample. With the increase of sintering time to 8 min, fine pores grew up and a group of larger pores appeared, as shown in Fig. 2(b). When sintering temperature was elevated, plentiful liquid phase appeared, the densification degree also increased and porosity (include pore size and amount) decreased, as shown in Figs. 2(c) and (d). The porosity reached the minimum at 1 350 ℃ when sintering for 8 min. From the images of porosity shown in Fig. 2, it is obviously revealed that sintered samples could not achieve full densification under appointed sintering process for nanohard phase Ti(C, N)-based cermet. When sintering temperature increased to 1 430 ℃, some cracks appeared on the external appearance, which were normal to axial direction. In addition, the amount and size of pores in the samples had some changes. Referring to Figs. 2(d) and (e), the size of large pores has not any change, but the amount manifolds, and a great deal of new small size pores emerge.

Hardness of samples sintered at various temperatures is listed in Table 3. The variation of hardness is consistent in the densification process. The maximum hardness only reaches HRA90,

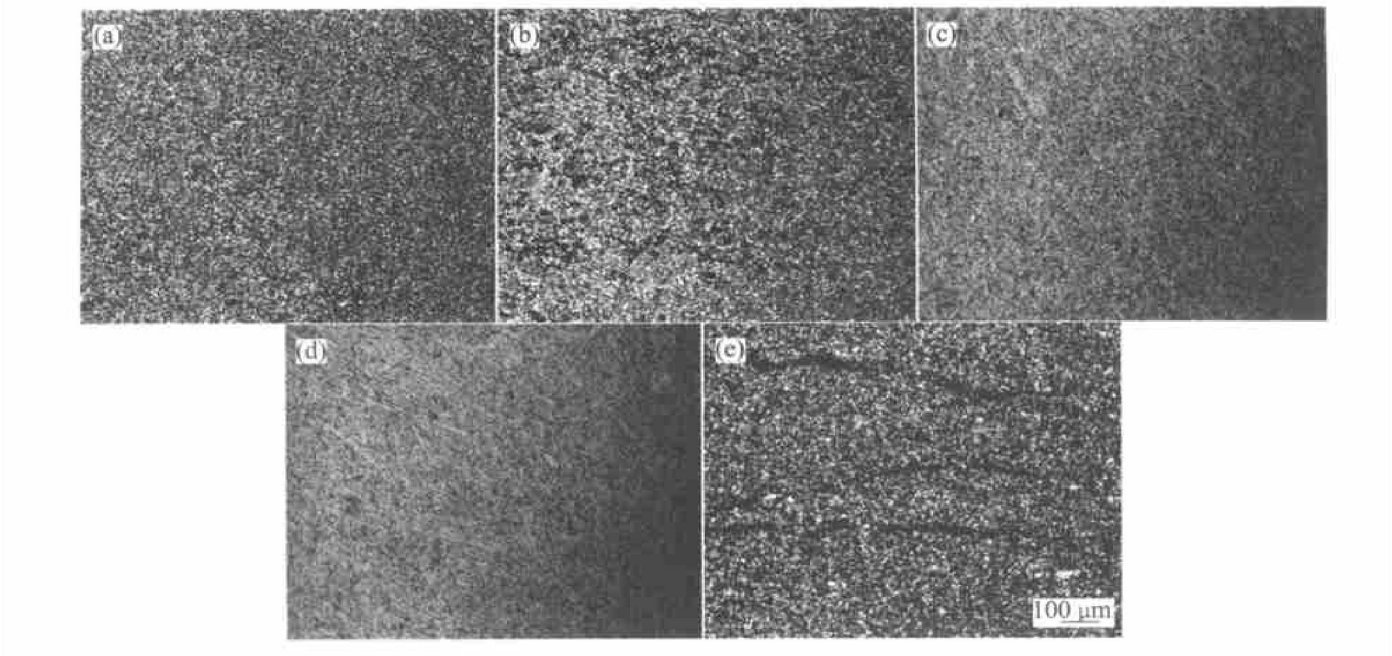

Fig. 2 Metallographs showing process of densification
(Black dots represent porosity and uncombined graphite)
(a) —1 050 ℃, 3 min; (b) —1 050 ℃, 8 min; (c) —1 200 ℃, 8 min; (d) —1 350 ℃, 8 min; (e) —1 430 ℃, 8 min

Table 3 Hardness of samples sintered with various processes

Processing parameter	1 050 ℃, 3 min	1 050 ℃, 8 min	1 200 ℃, 8 min	1 350 ℃, 8 min
Hardness (HRA)	67.4	70.6	84.6	90.2

which might be relative to the porosity and graphite phase morphology in samples.

3.2 Characterization of phase transformation

In order to understand the influence of SPS on phase transformation of nano hard phase Ti(C, N)-based cermet, X-ray analysis was used to identify present phase. Fig. 3 shows X-ray diffraction patterns of mixed powder and specimens sintered with various processes. The characterization of phase transformation for SPS nano hard phase Ti(C, N)-based cermet was summarized as follows:

1) The rate of phase transformation was much fast than that in conventional sintering. Due to the effect of surface purification and the mechanical pressure, SPS can provide higher sintering driving force than conventional sintering, and in addition to surface effect of nano particle, nano Ti(C, N)-based cermet should be of tremendous rate of phase transformation during SPS in theory, In fact, the results in experiment are also in favor of that.

Analyzed from Fig. 3, Mo reacted with free C to form Mo_2C, and Mo_2C rapidly dissolved and disappeared in short period of sintering at 1 200 ℃ for 8 min. Compared with conventional vacuum sintering[14, 16], the dissolution temperature of Mo_2C was

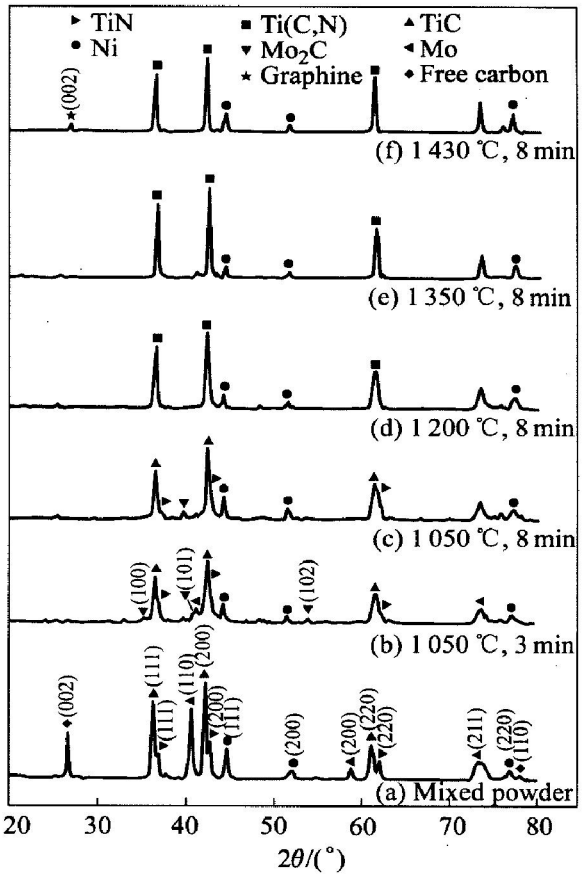

Fig. 3 X-ray diffraction patterns of mixed powder and specimens sintered with various processes

almost the same, but the period was greatly shortened.

TiN exhibits an especial behavior compared with that in conventional vacuum sintering. During conventional sintering, TiN has very high stability com-

pared with that of TiC, Mo_2C, WC and TaC, and it has very slow dissolution rate. However, during SPS, TiN completely dissolved when sintering at 1 200 ℃ for 8 min.

2) C in carbides had much more tendency of graphitization. The added free C had its corresponding peaks in the XRD pattern of mixed powders. During SPS, since it reacted with Mo and oxides on the surface of particles, and dissolved into binder, it was exhausted, as shown in Figs. 3(b), (c), (d) and (e), respectively. However, when being sintered at 1 430 ℃, the XRD peaks of graphite phase came forth, which manifested that there was fresh graphite phase formed during sintering.

Since TiN and TiC have the same sodium chloride structure, C super-lattice in TiC can be replaced by N atom to form continuous solid state Ti(C_{1-x}, N_x). Owing to the powerful sintering driving force and the effect of surface size of nano particle as well as little mass for single nano particle, TiN promptly dissolved into TiC or (Ti, Mo)(C, N) composite solid state, so TiN could not been detected in the specimens sintered at temperature above 1 200 ℃. The variation of lattice parameters of TiC and Ti(C, N) could also distinctly show the dissolution process of TiN. Fig. 4 shows a plot of the variation of lattice parameters of TiC and (Ti, Mo)(C, N) (called Ti(C, N) afterwards) and binder Ni. Below 1 200 ℃, The decrease of lattice parameter of Ti(C, N) was partially due to the dissolution of N into Ti(C, N).

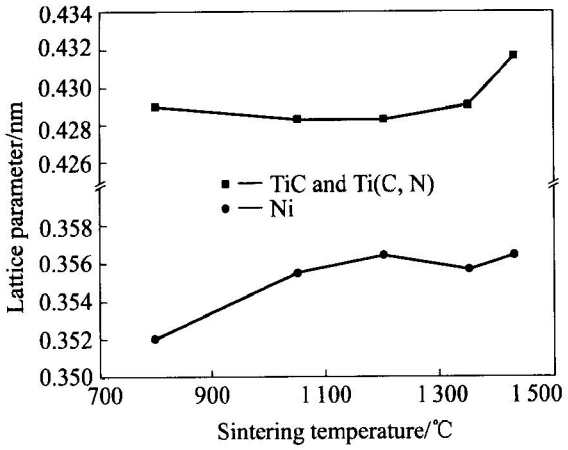

Fig. 4 Variation of lattice parameters of TiC, (Ti, Mo)(C, N) and binder with sintering temperature during SPS
(Data at 800 ℃ represents that of mixed powder)

In the temperature ranging from 1 200 to 1 430 ℃, a special variation occurred in the lattice parameter of Ti(C, N). For conventional vacuum sintering at temperature below 1 450 ℃, the lattice parameter of Ti(C, N) decreased all the while[17, 18]. However, for nano hard phase Ti(C, N)-based cermet sintered by SPS, the lattice parameter did not decrease but increased above 1 200 ℃. By comparing atomic radius of Ti(1.4318 Å), Mo(1.3626 Å), C (0.77 Å) and N(0.75 Å)[19], and taking the process of dissolution/reprecipitation of carbides into account, it could be concluded that the decrease of lattice parameter of Ti(C, N) resulted from the decomposition of N and C from Ti(C, N). Referred to the XRD pattern in Fig. 2(f), newly formed graphite phase was not detected. Decomposed C from Ti(C, N) graphitized to form graphite phase.

By associating the variation of porosity described above with the denitrification degree, which increased in the sample sintered at 1 430 ℃, it was affirmed that denitrification occurred above 1 200 ℃. The higher the sintering temperature is, the stronger the degree of the denitrification is. It is just the denitrification that forms N_2, generates gaseous paths and makes the porosity increase. The decomposition of C and N from Ti(C, N) brings about sintered samples not fully densed and limits the hardness of sintered samples.

3.3 Characteristics of microstructure

3.3.1 SEM observation

Fig. 5 shows the SEM micrographs of specimen sintered at 1 350 ℃ for 8 min. It is observed that the hard phase grains are uniformly embedded in the binder matrix, but the grain size is not uniform. The distribution of grain size is from less than 90 nm to 500 nm, most of them are about 200 nm. Compared with particle size of raw TiC of 90 nm, some grains grow up. On the whole, the grain growth was successfully controlled for SPS nano hard phase Ti(C, N)-based cermet. It was due to that, the period of sintering was so short that the process of dissolution/reprecipitation of carbide was effectively restrained and the formation of rim phase is reduced; and that the agglomeration of nano particles facilitated grain growth. Since SEM back scattered electron image is relative to the atomic number in phase, the contrast grade in hard phase of Fig. 5(b) might be used to approximately understand some phase transformation occurred during SPS. For SPS nano hard phase Ti(C, N)-based cermet, the hard phase grains has not the typical core-rim structure. It is once again indicates that the powerful sintering driving force provided by SPS and higher surface activity of nano particle promotes complete dissolution of TiC and TiN in each other in short time, resulting in no TiN remained acted as core phase.

3.3.2 TEM observation

Fig. 6 presents some TEM micrographs of specimen sintered at 1 350 ℃ for 8 min, showing different structural characteristics in specimen. Fig. 6(a) dis-

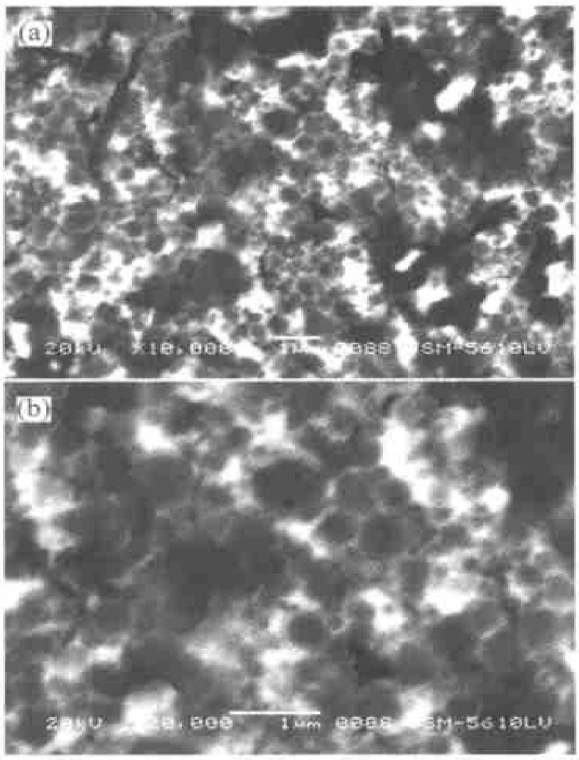

Fig. 5 SEM micrographs of samples sintered at 1 350 ℃ for 8 min
a) —Distribution and size of grain and dispersion of hard phase; b) — Microstructure of hard phase

plays the morphology of equiaxed grains come from agglomerated particles and recrystallization. The phase pointed by arrow in Fig. 6(b) is titanium oxide TiO_2 determined by SED as shown in Fig. 6(d), although XRD analyse could not identify it. The presence of TiO_2 demonstrates that the oxides on the surface of particles could not completely deduced for nano hard phase of Ti(C, N)-based cermet in short period sintering. The high-brightness band-like phase pointed by arrow in Fig. 6(c) is graphite determined by SED as shown in Fig. 6(e). Though XRD analyse could not detect it in the sample sintered at 1 350 ℃, it has already formed in fact.

Though SPS had a series of virtues and some successful exemplifications, it did not get satisfying results on microstructures and mechanical properties for the application of nano hard phase of Ti(C, N)-based cermet in present work. It should further be studied whether SPS is applicable to the materials such as Ti(C, N)-based cermet, in which some structure were not enough stable, especially there existed gaseous escape during sintering. Certainly, it should be envisaged that high oxygen content in raw powders was one of factors influencing sinterability in present work and the optimum process

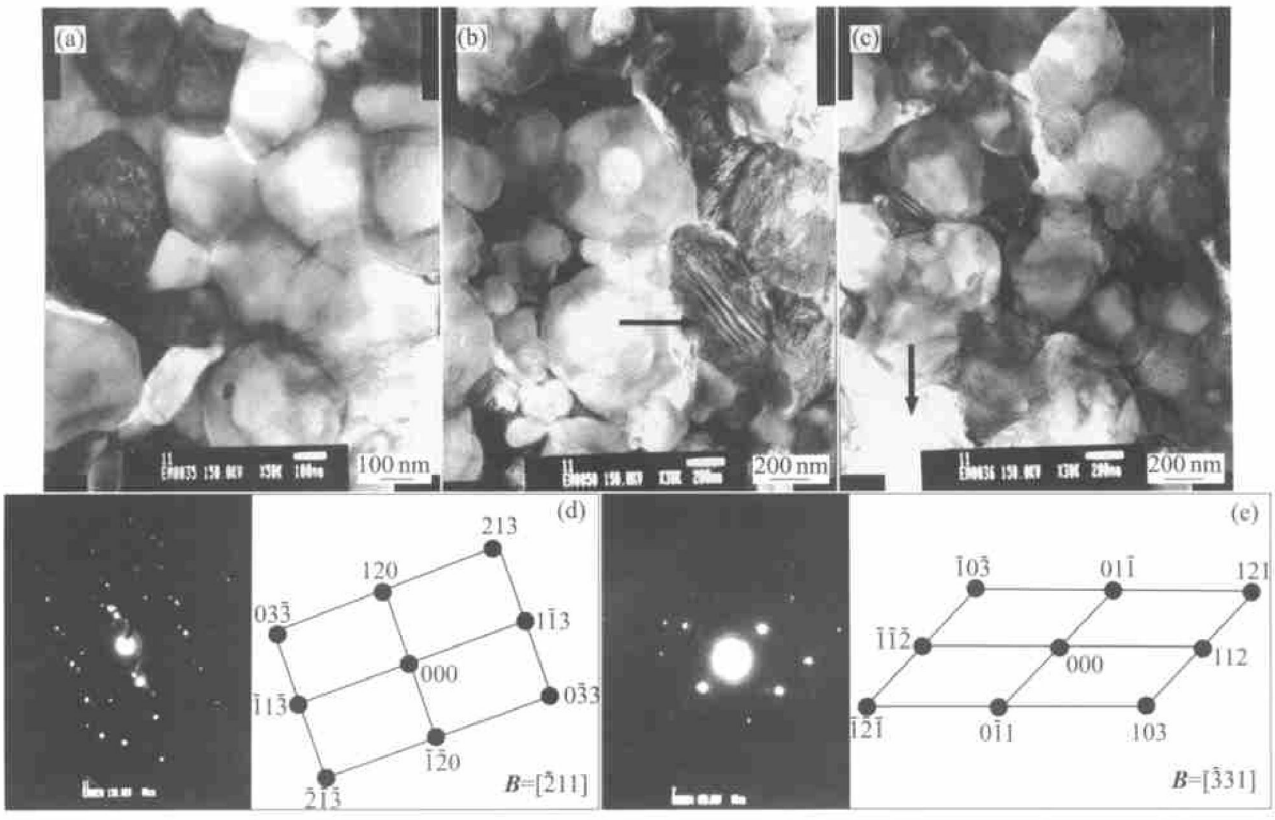

Fig. 6 TEM micrographs of sample sintered at 1 350 ℃ for 8 min
a) —Morphology of equiaxed grains coming from agglomerated particles and recrystallization; (b) —Morphology of TiO_2 pointed by arrow; (c) —Morphology of band-like graphite pointed by arrow; (d) —SED pattern of arrow pointed phase in (b) and its diffraction labeled graph; (d) —SED pattern of arrow pointed phase in (c) and its diffraction labeled graph

needed to be further investigated.

4 CONCLUSIONS

1) By means of SPS, nano hard phase Ti(C, N)-based cermet can be rapidly densified, however, due to denitrification from Ti(C, N), the full densification of the samples can not be obtained.

2) SPS can significantly accelerate the rate of phase transformation of Ti(C, N)-based cermet. When being sintered at 1 200 ℃ for 8 min, Mo_2C is completely dissolved. TiN represents different stability compared with that in conventional vacuum sintering. When being sintered at temperature above 1 200 ℃ for 8 min, TiN entirely dissolves into TiC or Ti(C, N) solid state. Above 1 200 ℃, Ti(C, N) composite solid state decomposes and C and N are separated out from Ti(C, N). N escapes in the form of N_2, and C is graphitized to form graphite phase.

3) The distribution of grain size of prepared Ti(C, N)-based cermet sintered at 1 350 ℃ covers a range of 90 nm – 500 nm, and most of them are 200 nm. SPS can not completely remove the oxides on the surface of particles and there exists titanium oxide TiO_2 in the sintered sample. Graphite phase is present in band-like shape in sintered sample.

REFERENCES

[1] Yamazaki K, Risbud S H, Aoyama H, et al. PAS(plasma activated sintering): transient sintering process control for rapid consolidation of powders[J]. Journal of Materials Technology, 1996, 56: 955 – 965.

[2] Omori M. Sintering, consolidation, reaction and crystal growth by the spark plasma system (SPS)[J]. Materials Science and Engineering, 2000, A287: 183 – 188.

[3] Nygren M, Shen Z. On the preparation of bio-, nano- and structrural ceramics and composites by spark plasma sintering[J]. Solid State Sciences, 2003, 5: 125 – 131.

[4] Gao L, Wang H Z, Hong J S, et al. SiC-ZrO_2(3Y)-Al_2O_3 nanocomposites superfast densidied by spark plasma sintering[J]. Nano Structured Materials, 1999, 11(1): 43 – 49.

[5] Cha S I, Hong S H, Kim B K. Spark plasma sintering behavior of nanocrystalline WC-10Co cemented carbide powders[J]. Materials Science and Engineering, 2003, A351: 31 – 38.

[6] Zhan G D, Kuntz J, Wan J, et al. Alumina-based nanocomposites consolidated by spark plasma sintering[J]. Scripta Materialia, 2002, 47: 737 – 741.

[7] Gao L, Wang H Z, Hong J S, et al. Mechanical properties and microstructure of nano-SiC-Al_2O_3 composites densified by spark plasma sintering[J]. Journal of the European Ceramic Society, 1999, 19: 609 – 613.

[8] Qiao L, Zhou H P, Li C W. Microstructure and thermal conductivity of spark plasma sintering AlN ceramics[J]. Materials Science and Engineering, 2003, B99: 102 – 105

[9] Wanga H J, Jina Z H, Miyamotob Y. Ti_3SiC_2/Al_2O_3 composites prepared by SPS[J]. Ceramics International, 2003, 29: 539 – 542.

[10] Sirirat R, Yukio M, Yoshiharu M. Microstructure and fracture toughness of a spark plasma sintered Al_2O_3-based composite with $BaTiO_3$ particulates[J]. Journal of the European Ceramic Society, 2003, 23: 1269 – 1276

[11] Kim H T, Kawahara M, Tokita M. Specimen temperature and sinterability of nickel powder in spark plasma sintering[J]. J Japan Sot Powder/Powder Met, 2000, 47(8): 887 – 891.

[12] Murakamia T, Komatsub M, Kitahara A, et al. Mechanical properties of spark plasma sintered strengthened by dispersion of Nb_2N phase of Mo and W[J]. Intermetallics, 1999, 7: 731 – 739

[13] Ettmayer P, Kolaska H, Lengauer W, et al. Ti(C, N) cermets—metallurgy and properties[J]. International Journal of Refractory Metals and Hard Materials, 1995, 13: 343 – 351.

[14] ZHENG Yong, XIONG Wei-hao. Microstructure and properties of micron and submicron Ti(C, N)-based cermets[J]. Materials Engineering, 2001, 5: 37 – 40. (in Chinese)

[15] Jeon E T, Joardar J, Kang S. Microstructure and tribo-mechanical properties of ultrafine Ti(CN) cermets[J]. International Journal of Refractory Metals and Hard Materials, 2002, 20(3): 207 – 211.

[16] Yoshimura H, Sugizawa T, Nishigaki K, et al. Reaction occurring during sintering and the characteristics of TiC-20TiN-15WC-10TaC-9Mo-5.5Ni-11Co cermets [J]. International Journal of Refractory Metals and Hard Materials, 1983, 2(4): 170 – 174.

[17] Zackrisson J, Rolander U, Andrén H O. Development of cermet microstructure during sintering[J]. Metallurgical and Materials Transactions A, 2001, 88(32A): 85 – 94.

[18] Zhang S Y. Titanium carbonitride-based cermets: processes and properties[J]. Materials Science and Engineering, 1993, A163: 141 – 148.

[19] Weast R C. Handbook of Chemistry and Physics[M], 70th Ed. Florida: CRC Press, 1989. 88 – 190.

(Edited by YANG Bing)